Research Article

Artur N. Gutkowski* and Zbigniew Cebulski

Analysis of Flame Propagation in Small Adiabatic Tubes Characterized by Different Degrees of the End Opening

https://doi.org/10.2478/mme-2021-0005
Received Sep 3, 2020; accepted Nov 21, 2020

Abstract: In the present work, we study numerically freely propagating flame in the stoichiometric propane-air mixture. The adiabatic small tubes with one end fully open and the second one characterized by different degrees of opening are examined. The degree of opening of the tubes was equal to: 0% (completely closed), 25%, 50%, 75% and 100% (fully opened) of the tube cross-sectional area. Several mechanisms, such as thermal expansion of the burned gas that can leave the tube freely (fully opened left end of the tube), frictional forces and movement of the unburned mixture generated by a pressure gradient, occur simultaneously during flame propagation. As a result, a nearly-exponential dependence of flame propagation speed as a function of time is observed. For fully open right end (100%), normalized flame speed reaches about 75–80 at the end of the tubes. By partially closing the right end, this effect is delayed and reduced – for 25% of the opening normalized flame speed is about 20 for all tube diameters.

Keywords: Premixed flame, small tubes, flame propagation speed, flame shape

1 Introduction

The study of the premixed flames propagating through the channels has a long history. The channel geometry and boundary conditions on the flame behaviour during its propagation was analysed first in [1, 2]. We can specify four typical configurations of flames propagating in the channels, which are schematically shown in the Figure 1.

The first configuration (Figure 1a) can be called a stationary flame. In this case, there is an inlet in which a premixed mixture with a certain velocity u_u (volume rate) is delivered, and an outlet where burned gas is evacuated (with velocity u_b). A flame is stabilized at some position in the tube. The second configuration (Figure 1b), we can call a moving flame. In this case, the ignition of the mixture is located at the open end of the tube and a flame propagates towards a close end, with flame propagation speed S_f in mixture, which is at rest ($u_u = 0$). The third configuration (Figure 1c) is similar to the previous one, it means that one end of the tube is open and another one is closed but a mixture is ignited at the closed end of the tube, therefore, $u_b = 0$. This configuration is very often used for turbulent flames and deflagration to detonation transition analysis. The last one (Figure 1d) is a channel opened at both ends.

The flame propagation in small channels has also been analysed numerically, for example, in the papers [3, 4]. The flame propagation mechanism in a tube with adiabatic and isothermal (cold) wall can be found in the paper [5], and for flames propagating between parallel plane walls in the work [6]. It was stated in these works that for tubes with

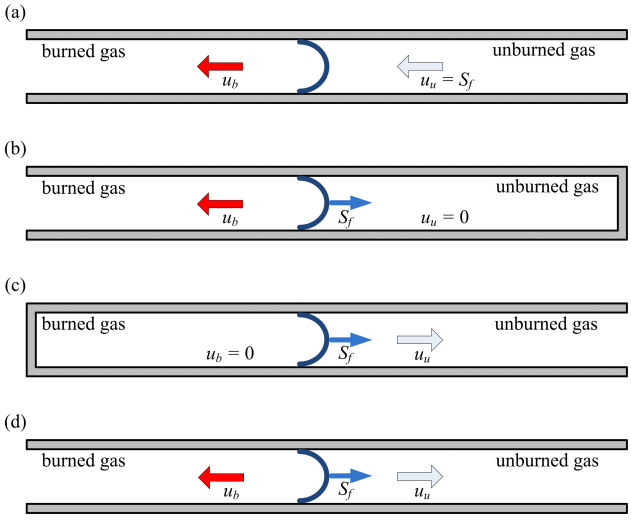

Figure 1: Typical configurations of flames propagating in channels.

***Corresponding Author: Artur N. Gutkowski:** Lodz University of Technology, Institute of Turbomachinery, Łódź, Poland; Email: artur.gutkowski@p.lodz.pl
Zbigniew Cebulski: Lodz University of Technology, Institute of Turbomachinery, Łódź, Poland; Email: zbigniew.cebulski@p.lodz.pl

adiabatic walls, the typical shape of the flame is a double-cusped partly concave ('tulip-shaped'), however, for tubes with isothermal walls, the shape of the flame is wholly convex ('mushroom-shaped' or 'finger-like'). In tubes with isothermal walls, it is also possible to form the tulip-shaped flame provided that the diameter of the tube is large enough. The flame propagation from a closed tube end to the open one was numerically analysed in [7] and the formation of a tulip flame was explained by a hydrodynamic process caused by the flame/wall interaction. The role of Lewis number *Le* on flame behaviour was considered in [8]. The authors used similar configuration to [7] and found that for $Le > 1$ flames accelerate slower as compared with $Le = 1$, and for $Le < 1$, flames acquire stronger distortion of the front and accelerate much faster than for $Le = 1$.

The tulip-shaped flame appears during deflagrations in closed pipes too [9].

There are many theories trying to explain which mechanisms are responsible for the formation of a tulip shape, for example, Darrieus-Landau instability, flame-shock interaction and deceleration of the finger-shape flame front. An extensive literature review presenting these mechanisms can be found in [10]. In the same work, propagation of hydrogen flames in a closed channel was also tested experimentally and numerically and the mechanism formation of the 'distorted tulip' flame was described.

A wide research concerning propagation and quenching of CH_4-air flames in small tubes, which takes into account the velocity profile and thermal boundary conditions on the walls of the tube can be found in [10]. The issue of the influence of the dead zone, that is, the distance between the flame and the tube walls, on the mixture flow passing through the tube and not subjecting to combustion was discussed.

Beside the tubes and channels with parallel plane walls, diverging channels on both sides [11] and a one-side narrowed channel [12, 13] were studied.

There are only a few works concerning freely propagating flames in a tube or channel open at both ends, schematically shown in Figure 1d. It seems that this problem has not been sufficiently examined yet. In work [14], the authors obtained the equations for the total travel time dependent on the length of the channel, which is independent of the Lewis number and the activation energy, except for their effect on laminar burning velocity S_L. A comparison of their results to the experimental results of [15] shows that the flame position as a function of time has a similar trend. The authors of [16] showed that during the early stages of flame propagation, the flame accelerates at an almost constant rate, independent of the channel height. If channels are sufficiently narrow, the flame retains constant acceleration until it reaches the end of the channel. In wider channels, however, the flame beyond a certain distance begins to accelerate at a nearly exponential rate, reaching exceedingly large speeds at the end of the channel.

The above summary shows that there is a lack of analyses in the literature presenting an effect of partial opening of one end of the tube (with simultaneous total opening of the other end at which the mixture is ignited) on the shape and speed of flames during propagation in small tubes. Therefore, it was decided to investigate numerically freely propagating flame in the stoichiometric C_3H_8-air mixture (equivalence ratio is equal to 1) in small tubes with an adiabatic wall.

2 Method and methodology

The present numerical study considers a flame freely propagating in an initially stationary mixture in the direction of gravitational acceleration. Figure 2 shows a schematic view of the geometry used during the numerical calculations. It consists of a circular tube with a diameter *d* and the length *L*. The length *L* along the axial direction equals twenty times the diameter ($L = 20d$). The diameter *d* was chosen to be 1, 2 and 3 mm, respectively. The operating pressure in a tube at the beginning of the calculations and outside is equal to 101,325 Pa. The mixture is ignited at the left end of the tube (always fully open). It takes place by extracting a part of the zone from the domain and assigning to it properties of hot combustion products, that is, temperature and chemical composition, to it (Figure 2). The second end of the tube is characterized by different degrees of opening. The degree of opening of the tubes was equal to: 0% (completely closed), 25%, 50%, 75% and 100% (fully opened) of the tube cross-sectional area. The boundary condition of the wall surface was modelled as an adiabatic and non-slip wall. A structured grid was used with elements not larger than 25 μm. As shown in [10], the grid size adopted in the present study has no practical influence on the laminar flame propagation speed. The domain was discretized with a Cartesian grid of 50×2000 points for the smallest tube and 60×2400 points for the biggest one, respectively.

The calculations are provided with several assumptions. First of all, the swirl velocity component is zero, meaning a symmetrical flow with respect to the centreline. Therefore, the case can be simplified to a 2D axisymmetric problem. To save the computation time, only half of the geometry is considered. Besides, other assumptions are made: there are no Soret and Dufour effects, there is no impact from the pressure and viscous forces. With the above

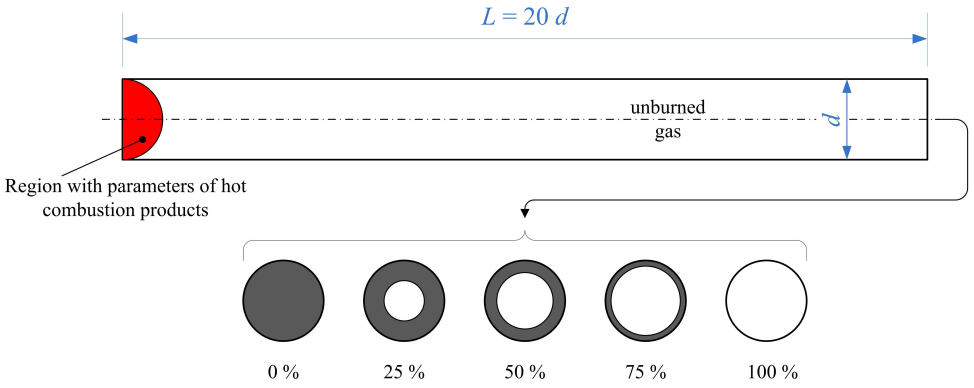

Figure 2: Schematic view of the geometry under analysis.

assumptions, the governing equations for the transient premixed flame can be written as follows:

Continuity:

$$\frac{\partial \rho}{\partial t} + \nabla \cdot (\rho u) = 0 \tag{1}$$

Momentum:

$$\frac{\partial}{\partial t}(\rho u_i) + \nabla \cdot (\rho u u_i) = -\frac{\partial p}{\partial x_i} + \nabla \cdot (\mu \nabla u_i) \tag{2}$$

Enthalpy:

$$\frac{\partial}{\partial t}(\rho h) + \nabla \cdot (\rho u h) = \nabla \cdot \left(\frac{k}{c_p} \nabla h\right) - \sum_{j=1}^{5} h_j^0 \omega_j M_j \tag{3}$$

Species:

$$\frac{\partial}{\partial t}(\rho Y_j) + \nabla \cdot (\rho u Y_j) = \nabla \cdot (\rho_j D_i \nabla Y_j) - \omega_j M_j \tag{4}$$

where u and u_i are the velocity vector and its composition in the axial and radial directions, and j for different species such as C_3H_8, O_2, CO_2, H_2O and N_2, respectively. The operating pressure, time, density, viscosity, thermal conductivity, diffusion coefficient, specific heat and enthalpy of the fluid are denoted by p, t, ρ, μ, k, D, c_p and h, respectively. The heat of formation, reaction rate (formation or destruction rate), molar weight and mass fraction of species j are respectively denoted as h_j^0, ω_j, M_j and Y_j. The fluid specific heat, thermal conductivity and viscosity are calculated as a mass fraction-weighted average of all the species. These properties for the individual species are determined from piecewise polynomials fit of temperature (for specific heat) and from kinetic theory for low-density gases (for thermal conductivity and viscosity). The kinetic theory relations are also used to evaluate the local mass diffusivity of the mixture. The fluid density is calculated using the incompressible ideal gas law:

$$p = \rho R_u T \sum_j \frac{Y_j}{M_j} \tag{5}$$

where R_u is universal gas constant.

A single-step irreversible reaction for C_3H_8-air combustion is as follows:

$$C_3H_8 + 5\,(O_2 + 3.76N_2) \rightarrow 3CO_2 + 4H_2O + 18.8N_2 \tag{6}$$

and the fuel consumption rate $\omega_{C_3H_8}$ is given by the Arrhenius formula:

$$\omega_{C_3H_8} = -A \exp\left(-E_a/R_u T\right) [C_3H_8]^m [O_2]^n \tag{7}$$

where the activation energy E_a is 1.256×10^8 J/kmol and the parameters m and n are 0.1 and 1.65, respectively, as recommended in [18]. The value of the pre-exponential factor A ($= 1.686\times10^{10}$ (kmol/m^3)$^{-0.75}$/s) from the fuel consumption rate equation was obtained from the numerical experiment in which we tried to find the calculated one-dimensional adiabatic flame speed consistent with the experimental data (41 cm/s, [19]).

The governing equations are discretized using the finite-volume method [20] and solved by Fluent. A second-order upwind scheme is used to discretize the governing equations and the SIMPLEC algorithm [21] is utilized for the pressure–velocity coupling. To solve the conservation equations, a 2D segregated solver with an under-relaxation method is used. The time step $\Delta t = 2\times10^{-6}$s was used in calculations. The solver first solves the momentum equations, then the continuity equation, and then updates the pressure and mass flow rate. The energy and species equations are subsequently solved and convergence is checked. The convergence criteria for the scaled residuals are set to be 1×10^{-5} for continuity, 1×10^{-6} for velocity, 1×10^{-5} for energy and 1×10^{-6} for species concentration.

The tube diameters can be presented in dimensionless form. Usually a flame thickness is used as reference, which can be defined as $\delta_T = D_T/S_L$, where D_T is the thermal diffusivity of the unburned mixture and S_L the laminar flame speed [14, 16]. A flame thickness for an adiabatic plane

flame equals to 0.05 mm. So the dimensionless diameters d/δ_T are 20, 40 and 60.

The normalized temperature was defined as where T_{ad} is an adiabatic temperature (= 2393 K). The reaction rate was normalized with the maximum reaction rate of an adiabatic flat flame as $\overline{\omega} = \omega/\omega_{\mathrm{ad,max}}$ ($\omega_{ad,max}$ = 3.50314 kmol/m^3/s).

3 Results and discussion

In the first considered case, flames propagated with fully closed right end of the tubes (0% opening). Shortly after ignition, the flame front is formed, and flame propagates further without any changes. Figure 3 shows a structure of the obtained flames.

For the tube with a 3 mm diameter, the flame shape is hemispherical (mushroom-shaped), while for smaller tubes, it is a concave (tulip-shaped). A mushroom-shaped flame in the 3 mm tube results from the 'round' ignition method used. The flames propagate with constant speeds within the given tube, which is shown in Figure 4, where a time history of the normalized flame position (x_f/L) in three tubes with a varying degree of opening at the right end is presented. For 0% of the opening, these relations are linear. The flame position is defined as the location of the maximum reaction rate along the centreline.

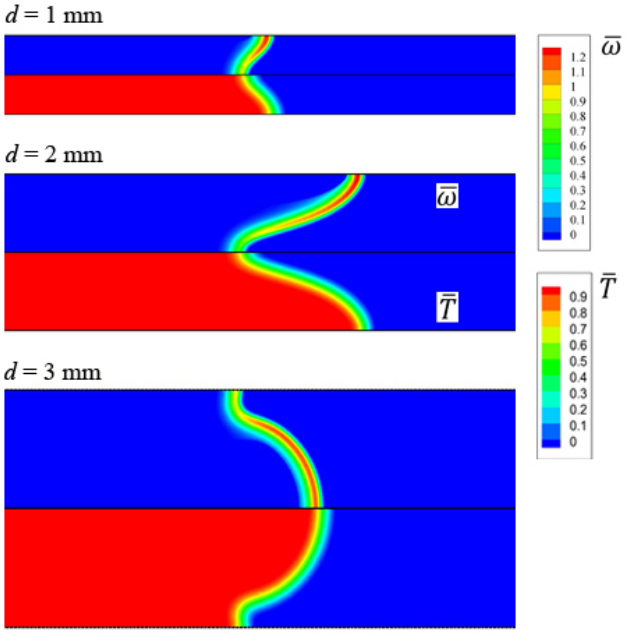

Figure 3: Distributions of the normalized reaction rate (top) and the normalized temperature (bottom) during flame propagation in tubes with the fully closed (0%) right end.

There is completely different behaviour if the right end of the tube is opened. Gradual increases of the opening of this end is followed by an increase in the steepening of the lines slope, but it is valid only for some period of time, where these relations are almost linear, after that inclinations of these lines increase sharply. The inclination is different, depending on the tube opening and its diameter.

The static pressure and normalized velocity profiles in the axial direction in a 2 mm tube at different flame locations is shown in Figure 5. If the right end of the tube is completely closed (0%), the flame acts as a piston and compresses the unburned gas Figure 5a. There is no pressure gradient ahead of the flame, it means there is no unburned gas motion towards a closed end as it is shown in Figure 5d. Whereas behind the flame (burned gas), pressure gradient is nearly constant and burned gas propagates in the opposite direction to the flame with constant velocity. As a

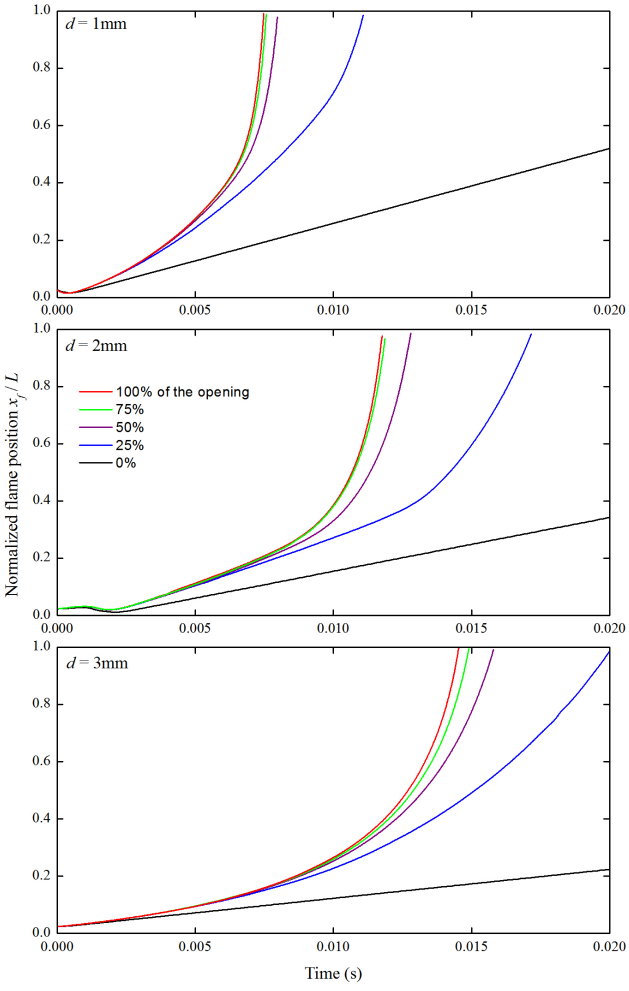

Figure 4: Flame position for different tubes and a varying degree of the right end opening versus time.

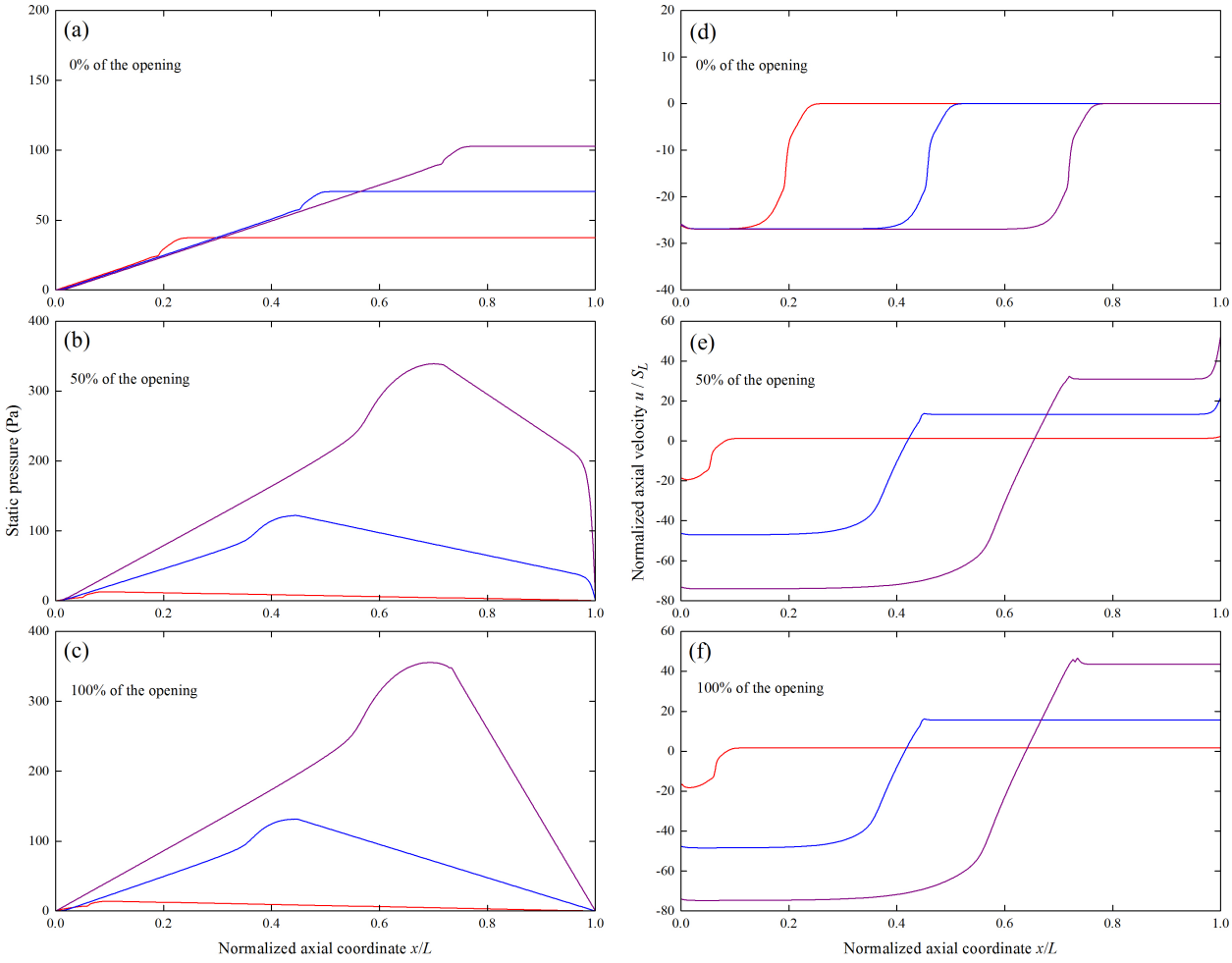

Figure 5: Axial static pressure and normalized velocity for three selected flame positions versus the normalized axial coordinate within the tube d = 2 mm for different degrees of the right end opening.

flame approaches the right end, the pressure in front of it – increases.

The total opening of the right end (100%) causes that a nearly constant pressure gradient appears ahead of the flame too (Figure 5c) and it drives the unburned gas to the right with the velocity that increases as a flame approaching the second end of the tube (Figure 5f).

By partially closing the right end, the unburned gas is not allowed to leave the tube freely, and some pressure drop appears (Figure 5b) in the vicinity of this end, which is accompanied with the velocity increase (Figure 5e). It is especially visible when the flame approaches the tube end.

To obtain the flame propagation speed, the flame positions have been differentiated. The flame speed S_f normalized by the laminar burning velocity S_L as a function of time is shown in Figure 6. As it was mentioned earlier, for all the tubes, the flame propagation speed is constant in fully closed (0%) tube at the right end. It is seen that flame propagation speed is negative in the first stage of the flame in the tube for 1 and 2 mm tubes (for all degree of opening). It relates to the ignition phenomena. At the initial period, a flame shape is convex towards unburned mixture, but just after it transforms into a tulip-shaped (concave) flame, during this process, the flame tip moves backwards. It is not visible for 3 mm tube, because a flame propagates with unchanged mushroom (convex) shape.

In the next stage, the normalized flame speed increases linearly to ~6 for 1 mm tube and ~4 for 2 mm tube. It is associated with the flame shape transformation – from concave to convex. This process is shown in Figure 7 for the tube with 2 mm diameter and 50% of the opening. During flame shape transformation, there is a moment when a flame takes a flat shape; later it begins to be hemispherical towards unburned gas.

Then the flame become elongated during propagation, which is accompanied by a transition from the hemispherical flame shape to a more convex one ('finger-like' shape). The time between each flame position, is 2 ms, except for

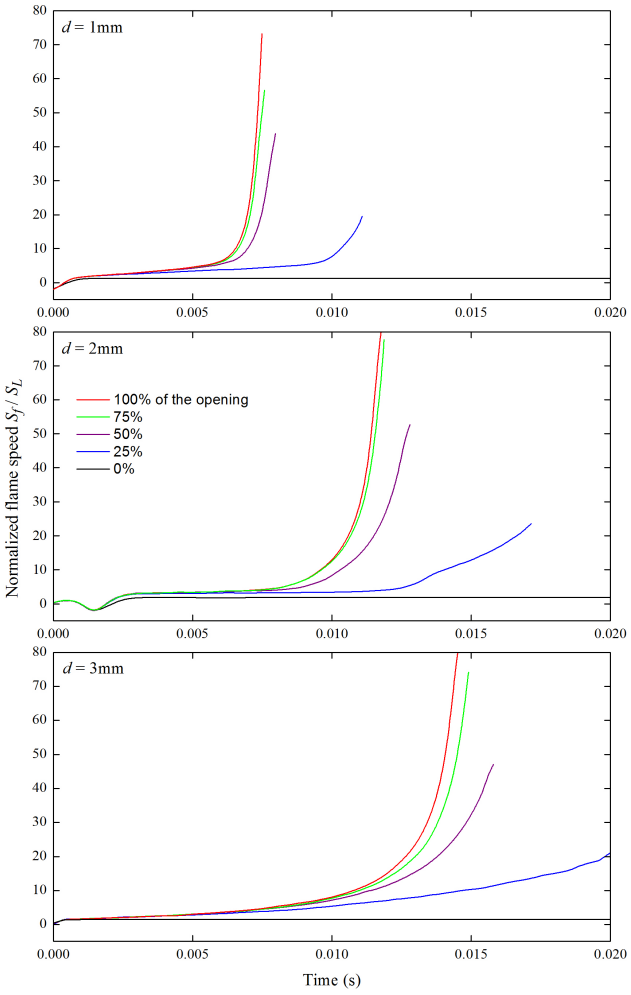

Figure 6: Normalized flame speed for different tubes and a varying degree of the right end opening versus time.

the last flame positions. For these cases, flame has reached the end of the tube earlier, therefore, we decided to show flames' locations spaced by smaller time period (0.8 ms). The position (and time) of the flame shape transformation depends on tube diameter and a degree of the right end opening. The smaller the opening, the farther (later) a flame transformation. After the flame shape transformation, its propagation speed increased at a nearly-exponential rate. As it is shown in Figure 7, an increase in normalized flame speed is associated with an increase in flame surface area.

In the case of a flame propagation in 3 mm tube, flame behaviour differs from the smaller tubes. As it was shown in Figure 3, a flame propagating in this tube is mushroom-shaped. Opening the right end does not cause transformation process from concave to convex as it is for smaller tubes, therefore, the change in flame propagation speed is a little smoother than for smaller tubes. During propagation, a

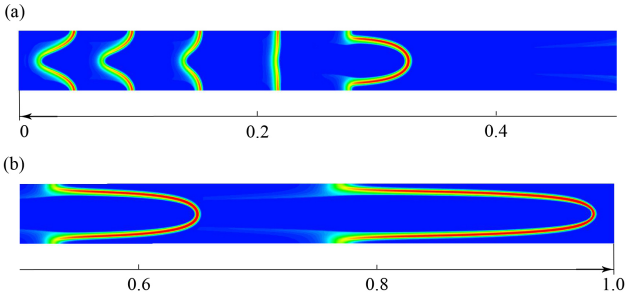

Figure 7: Illustration of the flame history (based on normalized reaction rate) during propagation in a tube (normalized by the *L*) with *d* = 2 mm for right end opening equal to 50%, where (a) is the first and (b) the second part of the tube. The time intervals are 2 ms, except the last two flames where it is 0.8 ms.

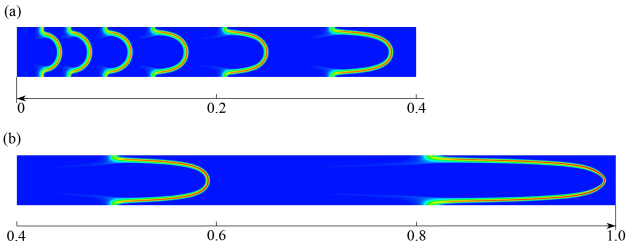

Figure 8: Illustration of the flame history (based on normalized reaction rate) during propagation in a tube (normalized by the *L*) with *d* = 3 mm for right end opening equal to 50%, where (a) is the first and (b) the second part of the tube. The time intervals are 2 ms, except the last two flames where it is 1.8 ms.

mushroom-shaped flame only elongates, as it is shown in Figure 8.

The maximum normalized flame speed at the tube ends is about 75–80 for all tube diameters and for fully open right end (100%). By closing the right end, we reduce normalized flame speeds, which for 25% of the opening is about 20.

The flame acceleration mechanism during its propagation in adiabatic tubes fully open in both ends is explained in [16]. Although tube diameters are wider in our work than in [16], it can be applied. Flame self-acceleration is an effect of combined actions of wall friction and thermal expansion. Due to the frictional forces at the wall of the tube, a flame becomes curved – a curved flame propagates faster than a planar one.

Thermal expansion causes that burned gas moves towards the left end of the tube. This movement sets a pressure gradient that pushes the unburned gas towards the right end of the tube (Figure 5c). A flame propagates in the unburned gas, which flows to the right (Figure 5f). Additionally, a curved flame is stretched, which results in elongation of flame surface, that increases flame propagation speed. By partially closing the right end, we introduce some restriction for flow leaving the tube. This leads to the appearance

of the pressure drop in the vicinity of this end and also reduces pressure gradient just ahead of the flame (Figure 5b). The result of the reduced pressure gradient is lower velocity of the unburned gas u_u (Figure 5e) and as a consequence lower flame propagation speed S_f.

4 Conclusions

Stoichiometric premixed C_3H_8-air flames propagating in adiabatic small tubes were examined. Flames propagate from a fully open end towards the second one characterized by different degrees of opening (from completely closed to fully opened). The degree of opening includes the tubes with: 0%, 25%, 50%, 75% and 100% cross-sectional area of the tube.

In the case of fully closed (0%) tube at the right end, the flame propagation speed is constant. If the right end is fully opened (100%), normalized flame propagation speed reaches about 75–80 at the end of the tubes. Normalized flame speeds are reduced by closing the right end, which for 25% of the opening is about 20.

For smaller tubes (1 and 2 mm) at the early stages of propagation, the flame speed varies almost linearly. At certain times, it changes dramatically and remains nearly-exponential relation. This behaviour relates to a flame shape transformation – from concave to convex one. This change is not so sharp for a 3 mm tube, because flame is convex from the beginning of its propagation.

References

[1] Mason W. and Wheeler R. V.: The Propagation of Flame in Mixtures of Methane and Air. Part I. Horizontal Propagation. *Journal of Chemical Society Transactions*, 117, 36-47, 1920.

[2] Guénoche G. in: Markstein G.: Non-steady Flame Propagation, Pergamon Press, Macmillan Company, Chapter E, 107–181, New York, 1964.

[3] Aly S. L., Simpson R. B. and Hermance C. E.: Numerical Solution of the Two-Dimensional Premixed Laminar Flame Equations, *AIAA Journal*, 17(1), 56, 1979.

[4] Aly S. L. and Hermance C. E.: A Two-Dimensional Theory of Laminar Flame Quenching, *Combustion and Flame*, 40, 173–185, 1981.

[5] Lee S. T. and Tsai C. H.: Numerical Investigation of Steady Laminar Flame Propagation in a Circular Tube, *Combustion and Flame*, 99, 484–490, 1994.

[6] Hackert C. L., Ellzey J. L. and Ezekoye O. A.: Effect of Thermal Boundary Conditions on Flame Shape and Quenching in Ducts, *Combustion and Flame*, 112, 73–84, 1998.

[7] Deng H. et al.: Numerical Investigation of Premixed Methane-Air Flame in Two-Dimensional Half Open Tube in the Early Stages, *Fuel*, 272, 1–11, 2020.

[8] Alkhabbaz M. et al.: Impact of the Lewis Number on Finger Flame Acceleration at the Early Stage of Burning in Channels and Tubes, *Physics of Fluids*, 31, 2019.

[9] Bi M., Dong C., Zhou Y.: Numerical Simulation of Premixed Methane-Air Deflagration in Large L/D Closed Pipes, *Applied Thermal Engineering*, 40, 337–342, 2012.

[10] Xiao H. et al.: Experimental and numerical investigation of premixed flame propagation with distorted tulip shape in a closed duct, *Combustion and Flame*, V. 159, 1523–1538, 2012.

[11] Kim N. I. and Maruta K.: A Numerical Study on Propagation of Premixed Flame in Small Tubes, *Combustion and Flame*, 146, 283–30, 2006.

[12] Akram M., Kumar S.: Experimental Studies on Dynamics of Methane–Air Premixed Flame in Meso-Scale Diverging Channels, *Combustion and Flame*, 158, 915–924, 2011.

[13] Jarosinski J., Podfilipski J. and Fodemski T.: Properties of Flames Propagating in Propane-Air Mixtures Near Flammability and Quenching Limits, *Combustion Science and Technology*, 174, 167–187, 2002.

[14] Gutkowski A.: Laminar Burning Velocity Under Quenching Conditions for Propane-Air and Ethylene-Air Flames, *Archivum Combustionis*, 26, 163–173, 2006.

[15] Kurdyumov V. N., Matalon M.: Flame Acceleration in Long Narrow Open Channels, *Proceedings of the Combustion Institute*, 34, 865–872, 2013.

[16] Mason W. and Wheeler R. V.: The Propagation of Flame in Mixtures of Methane and Air. Part I. Horizontal Propagation, *Journal of Chemical Society Transactions*, 117, 36–47, 1920.

[17] Kurdyumov V. N., Matalon M.: Self-Accelerating Flames in Long Narrow Open Channels, *Proceedings of the Combustion Institute*, 35, 921–928, 2015.

[18] Westbrook C. K. and Dryer F. L.: Simplified Reaction Mechanisms for the Oxidation of Hydrocarbon Fuels in Flames, *Combustion Science and Technology*, 27, 31, 1981.

[19] Law C. K.: Combustion Physics, New York, Cambridge University Press, 2006.

[20] Patankar S.V.: Numerical Heat Transfer and Fluid Flow, New York, McGraw-Hill, 1980.

[21] van Doormaat J. P. and Raithby G. D.: Enhancements of the SIMPLE Method for Predicting Incompressible Fluid Flows, *Numerical Heat Transfer*, 7, 147, 1984.